FDTD Analysis of Patch Antennas on High Dielectric-Constant Substrates Surrounded by a Soft-and-Hard Surface

RongLin Li, *Senior Member, IEEE,* Gerald DeJean, *Member, IEEE,* Emmanouil Tentzeris, *Senior Member, IEEE,* John Papapolymerou, *Senior Member, IEEE,* and Joy Laskar, *Senior Member, IEEE*

***Abstract*-- The surface-wave diffraction at the edge of a finite size substrate with a high dielectric constant is the dominant mechanism affecting the radiation pattern of a patch antenna fabricated on this material. A soft-and-hard surface (SHS) can be used to block the surface waves from propagating outward along the dielectric substrate, thus reducing the unwanted diffraction. Patch antennas surrounded by the SHS are analyzed using the finite-difference time-domain (FDTD) technique that implements the SHS boundary conditions using a simple modified subcell model. A square stacked-patch antenna and a circularly polarized (CP) patch antenna on a thick LTCC multilayer substrate are investigated. It is shown that the radiation pattern of the square patch on a big-size substrate can be significantly improved using SHS while the backward radiation level of the CP antenna with SHS on a small-size substrate is considerably reduced.**

***Index Terms*—Finite-difference time-domain (FDTD) technique, patch antennas, soft-and-hard surface (SHS).**

I. Introduction

The explosive growth of wireless communication systems has led to an increasing demand for integrated compact antennas. Thus, fabricating patch antennas on a high dielectric-constant substrate (such as GaAs or LTCC) is becoming attractive for miniaturized wireless modules. However, direct use of high dielectric-constant substrates with patch antennas results in strong surface-wave modes. The diffraction from these surface waves at the edge of finite-size substrates degrades the radiation pattern (containing dips near the maximum and significant backward radiation level) and reduces the radiation efficiency of the patch antennas [1].

For years, a number of techniques have been developed to improve the radiation patterns of patch antennas with high dielectric-constant substrates. The most popular method is to construct a periodic band-gap (or perforated) structure surrounding the patch antenna to prevent energy from being trapped in the substrate [2]-[3]. Unfortunately, to form a band gap in the substrate via periodic holes requires considerable area, which may make it impractical for some applications. Typically, to form a band gap at least three periods are required with a period being on the order of a wavelength. Another considered approach has been to lower the effective dielectric constant of the substrate under the patch to allow for more effective radiation [4]-[5]. The drawback of this approach is that the resultant patch antenna has to be larger than that on the unperturbed substrate, losing the advantage of using high dielectric substrate for reduction of antenna size.

Recently, the soft-and-hard surface (SHS) is becoming a hot active topic in the research of artificial electromagnetic surfaces. The concept of SHS originated from acoustics and introduced in electromagnetic theory in the 1980s [6]. As one of the basic boundaries in electromagnetics, the SHS is a mathematically idealization of a surface that is both electrically and magnetically ideally conducting in one direction defined by a real unit vector [7]. Such a surface can be realized by a combination of a perfect electric conductor (PEC) and a perfect magnetic conductor (PMC), a strip-loaded grounded dielectric slab, or a corrugated surface [8]. Also the SHS can be realized in high-dielectric constant substrates using standard processing techniques, such as the multilayer organic (MLO) or low temperature co-fired (LTCC) technology. The metalized walls of the corrugated surface can be substituted with rows of plated via holes that have been studied extensively both in terms of electrical performance as well as low cost fabrication aspects. For silicon substrates, micromachining techniques (e.g. wet or dry etching) can be implemented to create either trenches or via holes that can be metalized and provide the SHS characteristics. The improved performance that SHS structures provide in combination with the low cost processing techniques for their implementation, makes them extremely attractive for a wide variety of wireless applications.

The advantageous characteristics of the soft surface can be utilized to block the propagation of surface waves in a patch antenna, thus alleviating the diffraction at the edge of substrate. The patch antenna is surrounded by a substrate covered with an SHS that is formed as a soft surface in the outward direction. As a result, it would be difficult for surface waves to propagate from the patch to the substrate edge. In this paper, the SHS-surrounded patch antenna is analyzed using the finite-difference time-domain (FDTD) method. Since the electric and magnetic fields in Yee's leapfrog scheme are not co-located in space or in time, the straight implementation of an SHS for the FDTD method requires the introduction of a modified cell (note that both electric and

Manuscript received July 18, 2003; revised November 26, 2003. This work was supported by the Georgia Electronic Design Center, the NSF Career Award under contract #9964761, the NSF Packaging Research Center of Georgia Tech, and the NASA project under contract #NCC3-1015.

The authors are with the School of Electrical and Computer Engineering, Georgia Institute of Technology, Atlanta, GA 30332 USA (e-mail: rlli@ece.gatech.edu).

magnetic fields are enforced to be zero in one direction tangential to the SHS). A simple contour-path subscell model is introduced to overcome the difficulty. The null-field condition of the magnetic field component is enforced indirectly by modifying the updating equation for the tangential component of the electric field on the SHS. A square stacked-patch antenna and a circularly polarized (CP) patch antenna are investigated to demonstrate the usefulness of the modified FDTD code and the effectiveness of SHS on the radiation pattern improvement of patch antennas on high dielectric-constant substrates.

II. Patch Antenna Surrounded by SHS

Fig. 1 shows a patch antenna with arbitrary shape that has been fabricated on a finite substrate with a dielectric constant of ε_r and a thickness of h. The dielectric substrate is backed by a couple of metal cavities and surrounded by an SHS ring. The ideal SHS conditions can be enforced by the following symmetric boundary conditions for the electric and magnetic fields [7]

$$\hat{v}\cdot\vec{E}=0\,,\ \hat{v}\cdot\vec{H}=0 \tag{1}$$

where $\hat{v}$ is a unit vector tangential to the surface. In the direction parallel to $\hat{v}$, a hard surface, along which the density of power flow is maximized, may be realized, while in the direction transverse to $\hat{v}$ (say $\hat{t}$) a soft surface where the power flow is zero is present. This feature can be observed by projecting Poynting vector $\vec{S}=\vec{E}\times\vec{H}^{*}$ in the direction $\hat{t}$:

$$\begin{aligned}\hat{t}\cdot(\vec{E}\times\vec{H}^{*}) &= [\hat{v}\times(\hat{t}\times\hat{v})]\cdot(\vec{E}\times\vec{H}^{*})\\ &= (\hat{v}\cdot\vec{E})[(\hat{t}\times\hat{v})\cdot\vec{H}^{*}]-[(\hat{t}\times\hat{v})\cdot\vec{E}](\hat{v}\cdot\vec{H})^{*}\\ &= 0\end{aligned} \tag{2}$$

In order to prevent the surface waves from propagating outward, it is desirable for the configuration in Fig. 1 to have a soft-surface condition in the radial direction. Therefore we choose $\hat{v}=\hat{x}$ ($E_x=0$, $H_x=0$) and $\hat{v}=\hat{y}$ ($E_y=0$, $H_y=0$) respectively along the left-and-right sides and the front-and-back sides.

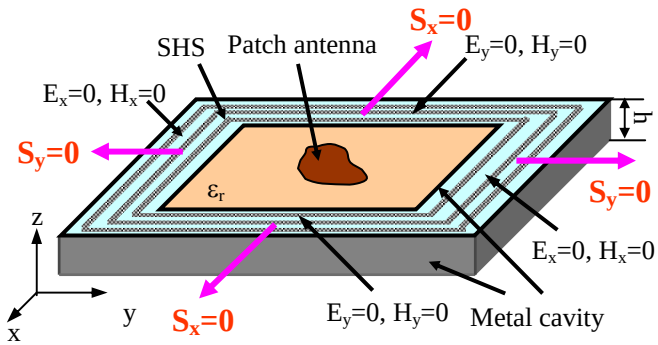

Fig. 1. Patch antenna surrounded by a soft-and-hard surface.

III. FDTD Modeling for SHS

To analyze the SHS-surrounded patch antennas using FDTD, the updating equations must be slightly modified since $\vec{E}$ and $\vec{H}$ components are not co-located in space and time in the Yee's algorithm, thus making it impossible to directly enforce the boundary conditions $\hat{v}\cdot\vec{E}=0$ and $\hat{v}\cdot\vec{H}=0$ simultaneously at same grid positions. In this paper we introduce a modified local subcell model to indirectly enforce the boundary condition for $\hat{v}\cdot\vec{H}=0$.

Without loss of generality, we assume $\hat{v}=\hat{x}$, that is, both $E_x=0$ and $H_x=0$ on the SHS. The boundary condition $E_x=0$ is directly enforced whereas $H_x=0$ is taken into account by modifying the updating equation for E_y. Consider a contour path C above the SHS and denote a space point on the SHS as $(i,j,K)=(i\Delta x,\,j\Delta y,\,K\Delta z)$, as shown in Fig. 2. Applying Ampere's Law along the contour C and assuming that $E_y\big|_{i,j,K+1/4}$ (at the center of the contour C) equals the average value of over the contour surface, we obtain [9]

$$\varepsilon_0\Delta x\frac{\Delta z}{2}\left(\frac{E_y\big|^{n+1/2}_{i,j,K+1/4}-E_y\big|^{n-1/2}_{i,j,K+1/4}}{\Delta t}\right)=\left(H_x\big|^{n}_{i,j,K+1/2}-H_x\big|^{n}_{SHS}\right)\Delta x + \left(H_z\big|^{n}_{i-1/2,j,K}-H_z\big|^{n}_{i+1/2,j,K}\right)\frac{\Delta z}{2} \tag{3}$$

Multiplying both side by $2\Delta t/(\varepsilon_0\Delta x\Delta z)$ and substituting $H_x=0$ on the SHS yields the following updating equation for $E_y\big|_{i,j,K+1/4}$:

$$E_y\big|^{n+1/2}_{i,j,K+1/4}=E_y\big|^{n-1/2}_{i,j,K+1/4}+H_x\big|^{n}_{i,j,K+1/2}\,2\Delta t/(\varepsilon_0\Delta z) + \left(H_z\big|^{n}_{i-1/2,j,K}-H_z\big|^{n}_{i+1/2,j,K}\right)\Delta t/(\varepsilon_0\Delta x) \tag{4}$$

The E_y component on the SHS $E_y\big|_{i,j,K}$ can be obtained through an extrapolation:

$$E_y\Big|^{n+1/2}_{i,j,K}=\frac{4}{3}E_y\Big|^{n+1/2}_{i,j,K+1/4}-\frac{1}{3}E_y\Big|^{n+1/2}_{i,j,K+1} \tag{5}$$

where $E_y\big|^{n+1/2}_{i,j,K+1}$ is the normal updating equation in the Yee's algorithm.

The modified updating equation for E_x on the SHS can be obtained in a similar way for $\hat{v}=\hat{y}$. Note that the field values at points beneath the SHS do not affect the FDTD solution since they are completely isolated by two PEC cavities and the SHS. The modified updating equations can be easily incorporated into any typical FDTD code.

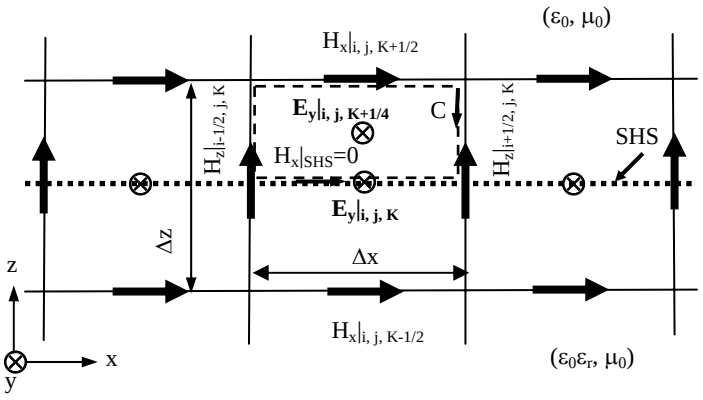

Fig. 2. Modified FDTD subcell model for SHS.

IV. Numerical Examples

Two numerical examples are investigated using the modified FDTD code. The first one, a stacked patch on a big-size substrate, is presented to demonstrate how to increase the forward directivity using SHS, while the second example, a CP patch on a small-size substrate, shows how the SHS can reduce the backward radiation level. Both patch antennas are assumed to use the LTCC multilayer material as their substrates whose dielectric constant is 9.5.

A. Stacked-Patch Antenna on a Big-Size Substrate

Consider a probe-fed square stacked-patch antenna on a thick big-size substrate surrounded by a square SHS ring whose width is denoted by w, as shown in Fig. 3. The size of the substrate is called thick and big because its thickness is more than half of the patch length and its lateral size is about 10 times of the patch size. The stacked-patch configuration is employed in such a thick substrate to reduce the length of the feed probe for a good input-impedance match. The number of the FDTD computational cells is 200 × 200 × 50 with a uniform cell size of 0.2 mm × 0.2 mm × 0.2 mm. Five uniaxial perfectly matched layer (UPML) cells are employed to truncate the FDTD computational region.

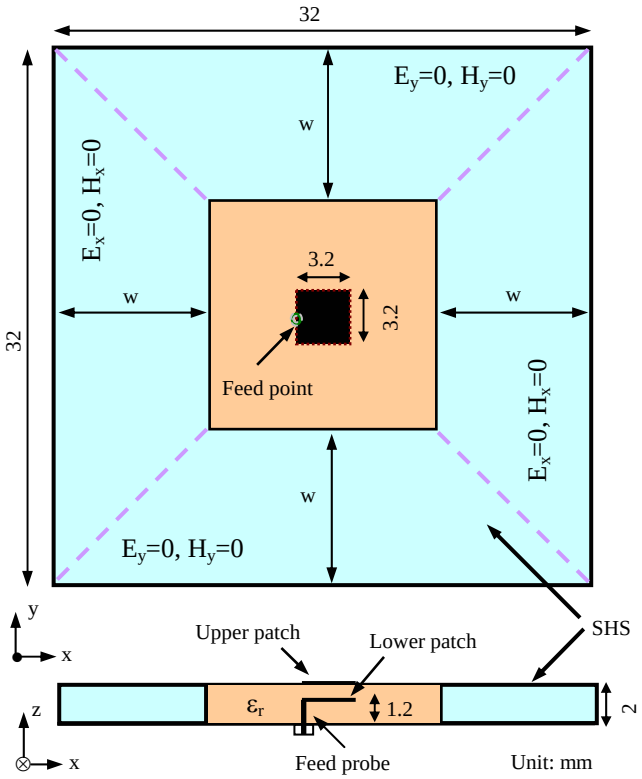

Fig. 3. Stacked-patch antenna surrounded by SHS.

For a patch antenna on such a thick big-size substrate with a high dielectric constant, its radiation pattern can be considerably degraded by the diffraction/scattering of the surface modes at the substrate edges. Fig. 4 shows the radiation pattern of the stacked-patch antenna at resonant frequency (10 GHz) when w=0 (i.e. without SHS). We can observe a dip (about –5 dBi) in the forward direction (the z direction) and a significant backward radiation level (about 0 dBi). The pattern degradation can be improved by introducing an SHS ring surrounding the patch antenna. Fig. 5 shows the directivity improvement in the z direction for different SHS ring widths. It is found that the directivity increases first as the width of the SHS ring becomes wider. But when the width further increases, the directivity gradually decreases due to shrinkage of the antenna aperture (the area for non-SHS). The maximum directivity is found to be 9.5 dBi at w=5 mm. The corresponding radiation pattern is shown in Fig. 6. It is observed that the backward radiation level is also significantly reduced (by more than 10 dB).

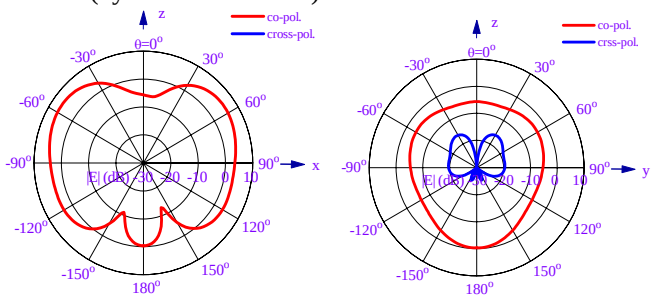

(a) (b)

Fig. 4. Radiation pattern for the patch antenna on a big-size substrate without SHS. (a) E-plane, (b) H-plane.

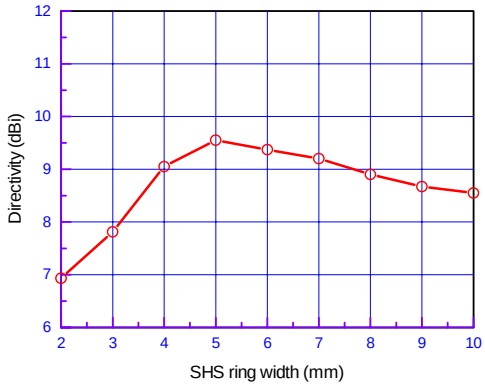

Fig. 5. Directivity improvement of the patch antenna surrounded by an SHS ring with different widths (w).

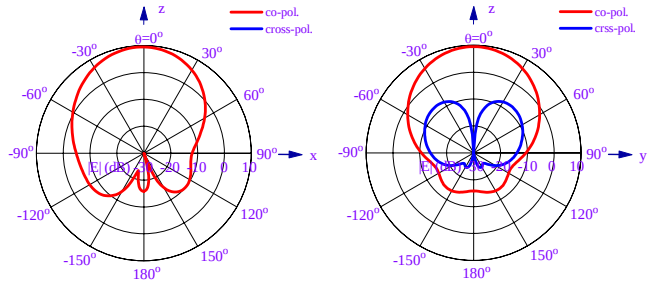

(a) (b)

Fig. 6. Radiation pattern for the patch antenna on a big-size substrate with SHS (w=5 mm). (a) E-plane, (b) H-plane.

B. CP Patch Antenna on a Smaller-Size Substrate for GPS Applications

For high-precision GPS applications, such as differential GPS, GPS-based spacecraft altitude determination or geometric surveying, the receiving antenna with a low-level backward radiation pattern is essential for the significant rejection of multipath signals. This property is particularly important for patch antennas because their backward radiation usually appears as a cross-polarized component. The multipath distortion results from the reflection of the GPS transmitted signal, which usually comes from the backside of the receiving antenna. As the GPS transmitted wave is right-hand circularly polarized (RHCP, or co-polarized), the directly reflected wave is left-hand circularly polarized (LHCP, or cross-polarized). Therefore, the patch antenna must have a lower cross-polarized component in the backward direction to alleviate the multipath effects. Here we demonstrate that an SHS can be used to reduce the backward radiation level while keeping a relatively small antenna size.

As shown in Fig. 7, a stacked-patch configuration is again employed. The antenna module is designed at the GPS civilian frequency (f_c=1575 MHz). The CP operation is realized by feeding the stacked-patch antenna on the diagonal axis of a square area 23.5 mm × 23.5 mm. The width of the SHS ring is chosen to be 12.5 mm to keep the total antenna size relatively small (only about 3 times of the patch size). In the FDTD model, a uniform cell size of 0.5 mm × 0.5 mm × 0.5 mm was used, which results in 200 × 200 × 60 computational cells.

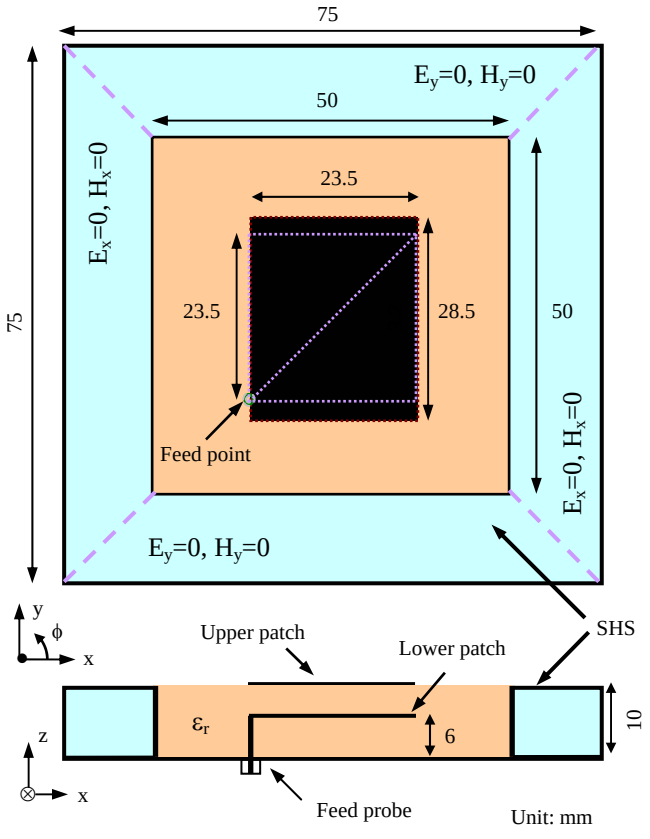

Fig. 7. CP patch antenna surrounded by SHS for GPS applications.

Fig. 8 shows the radiation patterns at f_c for the CP antennas with and without SHS for comparison. We can see that the backward radiation level (less than -15 dBi) of the patch antenna with SHS is about 14 dB lower than that without SHS. Note that a bigger ground plane (about 6-7 times of the patch size [10]) is needed for the similar low backward radiation level if without using SHS. The directivity gain (RHCP, E_R) is more than 0 dBi up to 15° elevation, much larger than the requirement of –5 dBi for maritime GPS applications [10]. Also the radiation pattern over the upper hemisphere (|θ|<90°) shows low cross polarization (LHCP, E_L, less than about -10 dBi) even though the SHS tends to slightly increase the cross-polarization level.

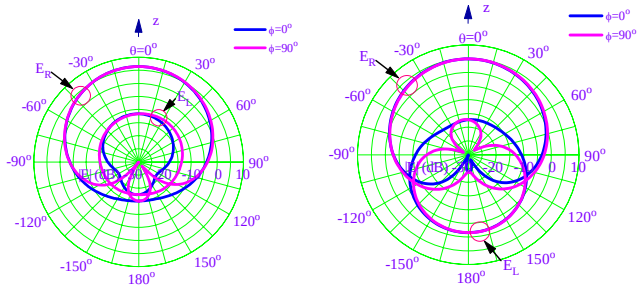

Fig. 8. Comparison of radiation patterns between the CP antennas with and without SHS. (a) with SHS, (b) without SHS.

V. Conclusion

The concept of soft-and-hard surface (SHS) is introduced to prevent surface waves from diffraction at the edge of high dielectric-constant substrates. Patch antennas surrounded by the SHS are analyzed using an FDTD model modified for the SHS boundary conditions. The numerical results verified the validity of the updated FDTD scheme and show that the SHS can effectively block the surface-wave propagation toward the edge of substrate, therefore leading to a significant improvement in the figures of merits for radiation performance, such as increased forward directivity and reduced backward radiation level.

References

[1] D. H. Schaubert and K. S. Yngvesson, “Experimental study of a microstrip array on high permittivity substrate,” *IEEE Trans. Antennas Propagat.*, vol. 34, pp. 72-97, 1986.

[2] R. Gonzalo, P. de Maagt, and M. Sorolla, “Enhanced patch-antenna performance by suppressing surface waves using phonotic-bandgap substrates,” *IEEE Trans. on Microwave Theory and Technique*. Vol. 47, no. 11, pp. 2131-2138, 1999.

[3] J. S. Colburn, Y. Rahmat-Samii, “Patch antennas on externally perforated high dielectric constant substrates,” *IEEE Trans. Antennas Propagat.*, vol. 47, no. 12, pp. 1785-1794, 1999.

[4] D. R. Jackson and J. T. Williams, and A. K. Bhattacharyya, “Microstrip patch designs that do not excite surface waves,” *IEEE Trans. Antennas Propagat.*, vol. 41, no. 8, pp. 1026-1037, 1993.

[5] J. Papapolymerou, R. F. Drayton, and L. P. B. Katehi, “Micromachined patch antennas,” *IEEE Trans. Antennas Propagat.*, vol. 46, no. 2, pp. 275-283, Feb. 1998.

[6] P.-S. Kildal, “Artificially soft and hard surfaces in electromangetics,”, *IEEE Trans. Antennas Propagat.*, vol. 38, no.10, pp. 1537-1544, 1990.

[7] I. V. Lindell, “Ideal boundary and generalized soft and hard conditions,” *IEE Proc. Microw. Antennas Propagat.*, vol. 147, pp. 495-499, 2000.

[8] Z. Sipus, H. Merkel, and P.-S. Kildal, "Green's functions for planar soft and hard surfaces derived by asymptotic boundary conditions," *IEE Proc. Microw. Antennas Propagat.*, vol. 144. no. 5, pp. 321-328, 1997.

[9] A. Taflove and S. C. Hagness, *Computational electrodynamics: the finite-difference time-domain method*, 2nd edition, pp. 411-472, Artech House, Inc., 2000.

[10] K. Fujimoto and J. R. James (Editors), *Mobile antenna systems handbook*, 2nd edition, pp. 568-580, Artech House, Inc., 2001.